Soft Robotic Module for Sensing and Controlling Contact Force

A. Buso[1], R.B.N. Scharff[1], E.L. Doubrovski[1], J. Wu[1], C.C.L. Wang[2] and P. Vink*[1]

***Abstract*— This work presents a soft robotic module that can sense and control contact forces. The module is composed of a foam spring encapsulated by a pneumatic bellow that can be inflated to increase its stiffness. Optical sensors and a light source are integrated inside the soft pneumatic module. Changes in shape of the module lead to a variation in light reflectivity, which is captured by the optical sensors. These shape measurements are combined with air pressure measurements to predict the contact force through a machine learning model. Using these predictions, a closed-loop control of the contact force was implemented. The modules can be applied to realize pressure distribution control in support devices such as seats and mattresses. The presented method is robust and low-cost, can measure both shape and contact force, and does not require (rigid) sensors to be present at the movable contact interface between the support device and the user.**

I. Introduction

The inherent compliance of soft robots makes them suitable for direct contact interaction with users. One promising application is to use soft robots as part of support devices such as seats and mattresses. For these products, the pressure distribution between the product and a user, resulting from the stiffness distribution in the contact area, is important for the experienced comfort. Especially regarding the seat pan, which supports the majority of the body weight, there is a correlation between pressure distribution and long term comfort (i.e., for 40 minutes of prolonged sitting or more) [1]. Research shows that the amount of pressure on an area of the body determines the compression of soft tissues and it should not be homogeneous for all body parts. Studies on seat comfort defined the preferred pressure distribution in different areas of a seat [1]–[3]. The biggest fraction of the load (49-54%) should be located at the rear part of the seat pan, around the ischial tuberosity. A lower load should be distributed to the middle part (10-28%) and the least load to the front part of the seat pan (6%), given the high sensitivity of the legs at that location.

The ideal pressure distribution can hardly be achieved by seats and mattresses with uniform stiffness. Therefore, the stiffness distribution of support devices is sometimes optimized using foam modules with different densities [4] (Fig. 1(a)). However, the variation in anthropometrics and weights demands for adaptability to accommodate various users. Providing a comfortable seating for different users requires the seat to be able to dynamically adapt its stiffness distribution for the individual needs. Furthermore, this capability of adaptation would allow to support the need of different pressure distributions for a user in different postures, or, in case of car seats, to account for changes in the vehicle acceleration [3].

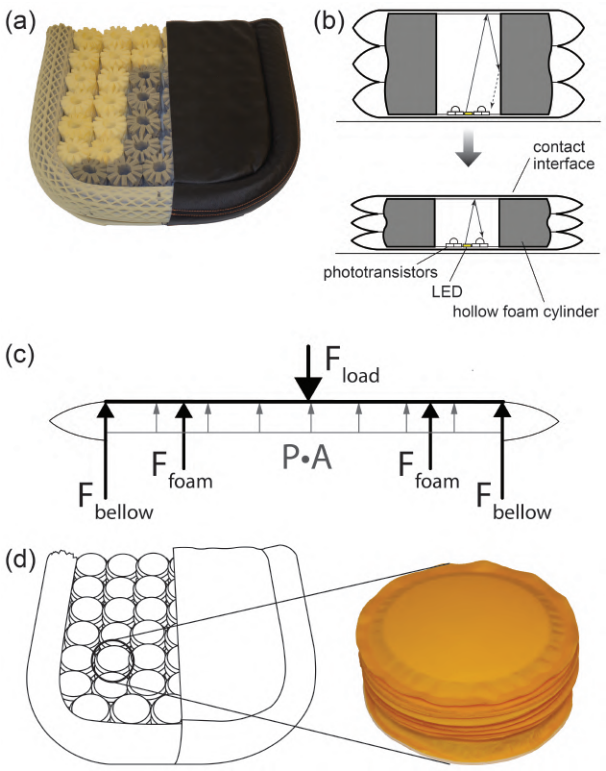

Fig. 1: (a) Inside of a seat with passive foam spring modules in different stiffness. (b) Working principle of the optical sensors used to detect deformation of the soft module: the light intensity increases when the module is compressed. (c) Free-body diagram of the contact interface. (d) Illustration of the envisioned implementation of the soft robotic module in a seat.

In this paper we present the development of a soft robotic module for the design of a programmable seat (Fig. 1(d)). This module has integrated sensors to measure the interface force (Fig. 1(b)), which serves for closed-loop control by adjusting its own stiffness through pneumatic inflation to reach a desired interface pressure. The module is composed of a hollow foam cylinder for passive stiffness, an air chamber that is pressurized to tune the contact force, and pressure and optical sensors, calibrated to measure the contact force. Combining multiple modules allows adaptations to the pressure distribution for varying users and use scenarios.

[1] A. Buso, R.B.N. Scharff, E.L. Doubrovski, J. Wu and P. Vink are with the Department of Design Engineering, Delft University of Technology, 2628 CE, The Netherlands.

[2] C.C.L. Wang is with the Department of Mechanical and Automation Engineering, The Chinese University of Hong Kong, Shatin, N.T., Hong Kong.

* Corresponding Author (E-mail: p.vink@tudelft.nl)

A. Related work

1) Soft Sensing: The control of highly under-actuated soft robots is challenging, especially when the system is confronted with unknown external loading. In these cases, the information about the actuation inputs is not sufficient to determine the state of the robot, and thus sensors are needed. Exterioceptive sensing methods such as cameras [5] are unable to measure the current state of a soft robotic seat while a person is sitting on it, as the sensors' view of the seat is obstructed. Proprioceptive sensing methods are necessary to overcome this problem. However, no off-the-shelf sensor is able to capture the high amount of *Degrees Of Freedom* (DOF) in soft robots while being flexible enough to accommodate their large deformations.

A modular soft surface making use of force sensitive resistors is presented by Robertson et al. [6]. Nonetheless, this sensor information cannot be used to predict the robot's shape. Moreover, the sensors are relatively expensive and have to be integrated on top of a moving module. Alternative methods have focused on integrating proprioceptive sensing capabilities to the soft material itself, such as capacitive sensing [7], piezoelectric sensing [8], sensing through optical waveguides [9], [10] and resistive sensing using liquid metal [11] or carbon nano-tubes [12]. A challenge of integrating the sensors directly into the soft material is the fabrication complexity and durability of such soft robots. To overcome this problem, sensors that measure changes in light resulting from changes in the actuator's shape are being used in soft robots [13], [14]. The soft body now acts as a signal generator and optical sensors are strategically placed inside the robots body to capture these changes in color and/or reflectance. This sensing approach has been applied in sensing of soft surfaces/skin [15]–[18], fingertips [19], [20], soft bending actuators [13], [14] and stuffed objects [21]. Cameras can be used as optical sensors [16]–[20], but are expensive, too big to be integrated in many soft robots, and require computationally expensive data processing. A relatively low amount of small and low-cost sensors such as photo-diodes [13], [14] and photo-transistors [15], [21] have shown to be sufficient to predict complex deformations, while being easy to integrate in soft robots. The relation between the deformation and sensor values can be modeled [17], [18], [20] or learned through machine learning [14]. In this work, the measurements of photo-transistors are used to give an indication of the shape of the bellow. By combining these shape indicators with the air pressure at which this shape is realized, the contact force can be accurately learned through a machine learning model.

2) Control of soft actuators: Closed-loop control for soft robots is challenging in general, even when the state of the soft robot is accurately measured. This is due to the small number of actuation inputs and the large amount of output DOFs in soft robots. The relation between the actuation inputs and deformation can be highly nonlinear [14]. It may be unclear what actuation strategy should be applied to achieve a desired state, and whether the desired state is achievable under the current loading. We follow the idea to reduce the complexity of this relation by limiting undesired DOFs of the actuator [22] and by limiting the possible load cases. For seats, the load is always applied on top of the actuator. Using stiffening actuators, the force on top of the actuator can be expected to increase monotonically with an increase in actuation power, allowing the use of PID control to close the control loop. Stiffening of soft actuators can be achieved in multiple ways, such as particle jamming [23]–[25], layer jamming [26], heating and cooling of shape memory polymers [27], or antagonistically arranged actuators [28]–[30]. An overview of stiffening in soft robotics is given by Manti et al. [31]. Contact force can not only be increased through an increment in stiffness, but also in deflection. In this work, the contact force is controlled by inflating a soft linear bellow. The unloaded length of the actuator (i.e., without external load) is changing with a variation in air pressure, influencing the deflection even when the length of the loaded module is kept constant. Therefore, this work refers to controlling the contact force, which can be converted to contact pressure for any given module layout.

B. Overview & organization of the work

This paper describes the design, fabrication, and control of a soft robotic module for achieving a prescribed contact pressure in support devices such as seats and mattresses. The module contains a hollow cylindrical foam structure for passive stiffness, and additionally uses air pressure in an embedded chamber to increase the module's stiffness. A light source and four photo-transistors are placed inside the cylindrical foam, at the bottom of the module, which is opposite to the contact interface. The measurements of the optical sensors and the air pressure inside the chamber are used to predict the force on top of the module using machine learning. Note that air pressure alone is not sufficient to predict the force on top of the bellow, as $\mathrm{F_{bellow}}$ and $\mathrm{F_{foam}}$ are unknown (see Fig. 1(c)). Therefore, additional information about the shape of the actuator is needed to accurately predict the load. The use of such optical sensing method to measure the shape of an object has recently been demonstrated by Scharff et al. [14]. As the same authors suggest, this work confirms that accurate proprioception can be achieved solely through changes in light reflectivity and without the presence of a color signal. In this study, we demonstrate that the shape indicators from the optical sensors and the air pressure combined provide sufficient information to accurately predict the load. Lastly, we further show that the sensor information can be used in a closed-loop control system towards an adaptive seat optimized for comfort.

The work is organized as follows: Section II explains the working principle and the fabrication method of the variable-stiffness soft module. The data collection is presented in Section III-A, followed by the data processing and training of the neural network (Sec. III-B). The results of the training and application in a closed-loop control system are discussed in Section IV. Lastly, limitations and future work are discussed (Sec. V).

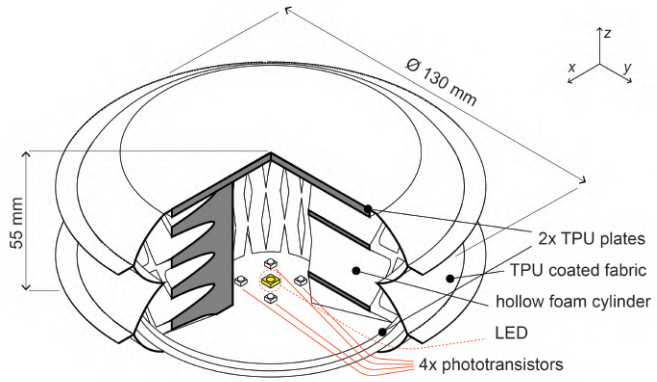

Fig. 2: Design of the soft robotic module. The module consists of a foam cylinder encapsulated by a bellow. Four photo-transistors and an LED are placed at the bottom of the module on the inside of the foam module.

II. Design

A. Overview

An illustration of the design of the soft robotic module is shown in Fig. 2. This module is intended to be part of a matrix that constitutes a seat pan (Fig. 1(d)). The goal is to control the distribution of the contact pressure across the seat surface by varying the stiffness or height of each module as previously done by Robertson et al. [6]. A hollow foam cylinder provides a passive stiffness to the module. Four photo-transistors are concentrically placed at the bottom of the module, on the inside of the hollow foam cylinder. An LED is fixed in the centre. The light emitted is diffused inside the hollow cylinder and reflected by its walls. When the cylinder is compressed along the z-axis less light is absorbed by the walls. The phototransistors output a voltage drop across a series resistor in reaction to an increment of light intensity (see bottom plot of Fig. 3). Non-axisymmetric loadings result in an uneven change of light intensities across the sensors.

The light measurements are combined with an air pressure measurement to predict the contact force on top of the module. The foam cylinder is encapsulated by a pneumatic bellow. The top and bottom of the bellow are connected to the foam. The more regular shape of the hollow foam cylinder simplifies the relation between the shape of the actuator and the optical measurements as compared to measuring light reflection in a module without the hollow foam cylinder. Hereby, the required number of training samples is reduced. When the module is pressurized, it expands in the z-direction (Fig. 1(b)). Obstructing this expansion creates a contact force.

B. Materials and fabrication

A mounting plate for the sensors was 3D-printed on an *Ultimaker 3+* using *Thermoplastic Polyurethane* (TPU) with shore value of 95A. The mounting board is equipped with the following components:

- Monotonic unidirectional light source (LED) placed at the centre of the mounting plate.
- Four photo-transistors in a square formation with equal distance (15 mm) from the LED.
- A 6 mm PVC tube inserted through the bottom plate for inflating the module.

The wiring was passed through the outlet tube. A *differential analog pressure sensor (MPXV5050G)* connected to the tube was used to measure the air pressure inside the module. The cylindrical bellow structure (130 mm diameter) was fabricated using Nylon fabric with a coating of TPU on one side (170 den, 275 $\mathrm{g/m^2}$, *ExtremTextil*®). The fabrication process of the bellows is described by Yang & Asbeck [32]. Rings of two different sizes were laser-cut from the fabric. The overlapping rings were stacked, with the TPU surfaces facing each other. The TPU surfaces were welded together in a heat press machine at 200° C. The bottom of the bellow was sealed to the 3D-printed TPU sensor mounting plate using a heating iron. A 50 mm high *Octaspring* [4] hollow foam cylinder was glued to the mounting plate. Octaspring is a lightweight hollow foam cylinder with a structure that gives it spring-like behavior. The cylinders are available in different densities in order to create a specific stiffness distribution in support devices (see Fig. 1(a)). The product is commonly applied in (aircraft) seats and mattresses. After inserting the Octaspring in the bellow, the module was sealed by welding a 3D-printed TPU layer on top of it.

III. Calibration

A. Data collection

The data acquisition process is illustrated in Fig. 3. The module was mounted underneath a 500 N load cell on a *Zwick/Roell Z*010 tensile testing machine. Steel L-shaped profile plates were clamped inside the upper and lower grips, to distribute the applied force equally across the module. All data were collected at a fixed displacement rate of 1 mm/s. Each experiment was initiated by inflating the module to a fixed pressure. Two *Arduino UNO* boards were utilized. The first board controlled the air pressure inside the module using an air pressure sensor and a small air pump. The second one stored the sensor values. The pump was shut off after reaching the starting pressure, allowing the air pressure to build up in the module when the load was being applied. The peak force at which the experiment was shut off ranges from 7 to 140 N in increments of 7 N. This was done for an initial air pressure ranging from 0 kPa to 3 kPa, with increments of 1 kPa. The maximum contact pressure on an automotive seat pan should be 18 kPa [2], which corresponds to 140 N on a module of 130x130 mm. The force data were collected using *TestXpert II* software at a frequency of 500 Hz. The data from the optical sensors and the air pressure sensor were collected at a frequency of 26 Hz with an *Arduino UNO* controlled from Matlab through serial communication. In order to align the force data with data from the optical and pressure sensors, an analog reference was created by applying a 20 N peak load prior to each experiment. The light sensor signals show a limited range of variation especially for tests with initial air pressure larger than 0 kPa (see Fig. 3). This is because at higher internal pressure the actuator compresses less.

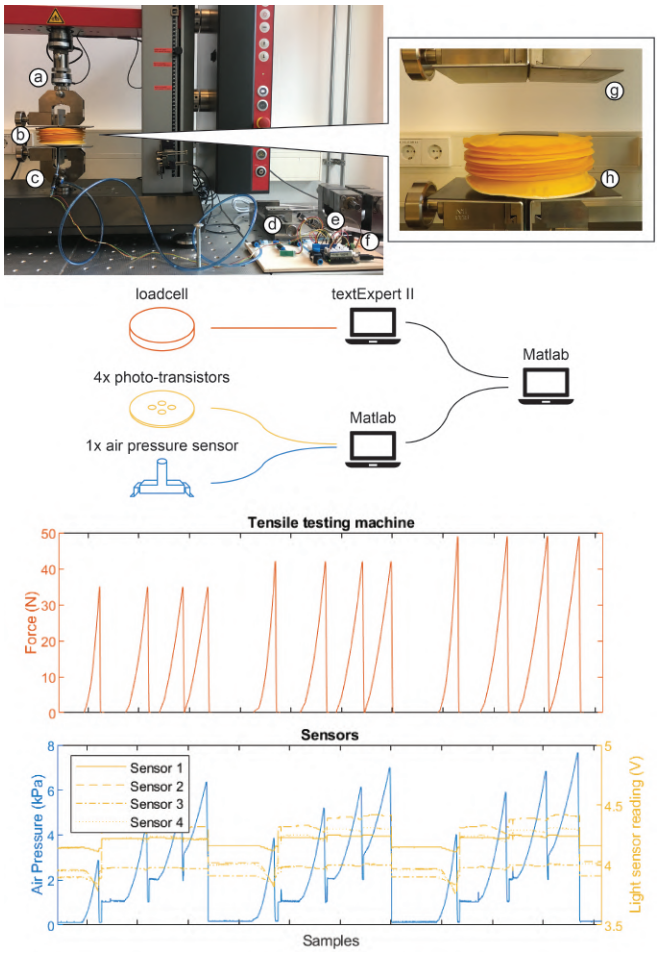

Fig. 3: *Top:* Experiment setup. (a) Load cell of the tensile testing machine. (b) Soft actuator. (c) Outlet tube. (d) Air pressure sensor (e) Air pump. (f) Arduino boards. (g) L-shaped profile plates. (h) Photo-transistors (inside the actuator, at the bottom). *Bottom:* Subset of training data for 3 sets of 4 measurements each (after processing).

A total of 68075 samples was acquired. The sampling distribution is shown in Fig. 4. It can be observed that for a certain air pressure there can be multiple contact forces.

B. Data processing

This section discusses how the raw data were processed in order to obtain the training data. First, the raw sensor data and contact force data were aligned by matching the peak in force and sensor values generated by the 20 N peak force that initiated each of the experiments. Then, the high frequency force data (500 Hz) were linearly interpolated at the sensor data points (26 Hz). The first 30 samples of the aligned data of each experiment were deleted to prevent inclusion of data from the 20 N peak. As it took some time for the upper grip to make contact with the actuator, a significant segment of the remaining data collected consisted of no-contact samples. Since inclusion of too many identical samples is not helpful and might bias the learning process, a random 90% of the no-contact samples were removed. The final dataset used for training and testing the machine learning models consisted of 42220 samples with the contact force ranging from 0 to 140 N and the air pressure ranging from 0 to 3 kPa.

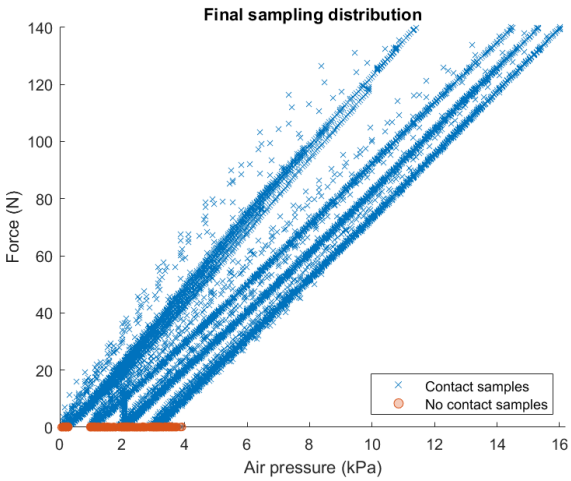

Fig. 4: Final sampling distribution. The 35.60% of the entire data set consisted of no-contact data, acquired when the force gauge was not in contact with the actuator. For the sensors calibration, all contact samples and only 10% of the no-contact samples were used.

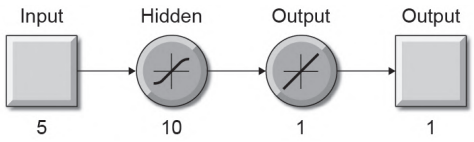

Fig. 5: Diagram of the FNN. The five inputs of the neural network are the measurements of the air pressure sensor and the four photo-transistors. The output is the contact force.

A multiple linear regression, a *Feed-forward Neural Network* (FNN) and a *Support Vector Regression* (SVR) were used to model the relationship between the sensor readings and the contact force. A single two-layer FNN with 1 hidden layer and 10 neurons was created (Fig. 5). The hidden layer applies a sigmoid transfer function and the output layer applies a linear transfer function. The Levenberg-Marquardt backpropagation algorithm was used to train the network with a total of 5 inputs (4 light values and 1 pressure value) and 1 output (contact force value). For all regression models, a randomly selected 85% of the samples was used for training set and the remaining 15% was used for testing.

IV. Results

A. Training

The best predictions were obtained using an FNN with *Mean Square Error* (MSE) of 4.73 on the test set (see Fig. 6). The multiple linear regression has MSE of 18.12 and the SVR of 23.18. It can be noticed that the accuracy of the FNN predictions increases at larger external forces.

When plotting the targets against the predictions of the SVR, several lines can be distinguished. Although the accuracy of these lines are off in terms of trueness, the precision of the predictions within each line is higher than the precision seen at the FNN. This suggests that there is an additional parameter of influence that is not fed into the training model,

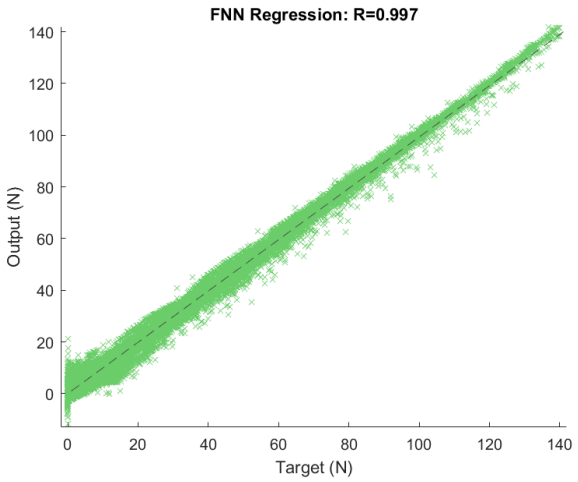

Fig. 6: Predicted contact force vs actual contact force from the FNN regression model, with values expressed in N. The dashed line represents the perfect regression line.

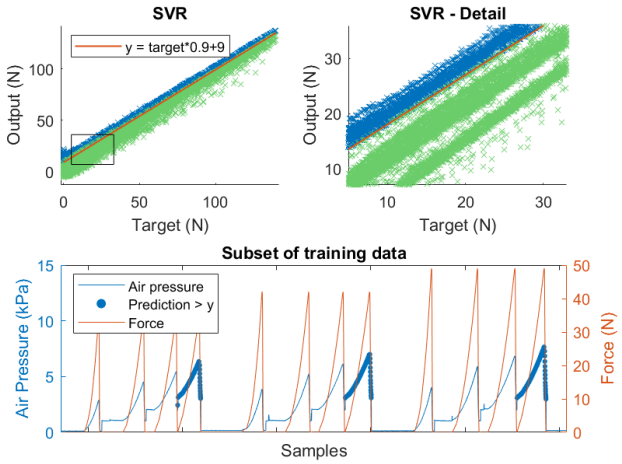

Fig. 7: *Top left:* Predictions of the SVR regression model. The samples above the red threshold line are indicated in blue. *Top right:* Zoomed-in view of the SVR. *Bottom:* Same subset of training data as Fig. 3. The samples above the red threshold line are indicated by blue dots.

as for example time-dependent material behavior in the bellow and the foam. The distinguishable lines correspond to the different set starting pressures in the experiments, as shown for one of the lines (indicated in blue) in Fig. 7. Due to nonlinearities, a nonlinear regression model will provide a more accurate prediction.

B. Closed-loop control

The FNN model was evaluated by using it in a closed-loop control system. The closed-loop control system was implemented using a PID controller. The block diagram of this system is shown in Fig. 8. An Arduino Uno was used to read the values from the photo-transistors and pressure sensor. The measured values were sent to a PC using serial communication. Using Matlab, the sensors data were converted by the trained FNN into a predicted contact force.

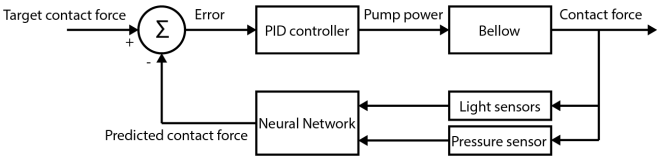

Fig. 8: Block diagram of controller system.

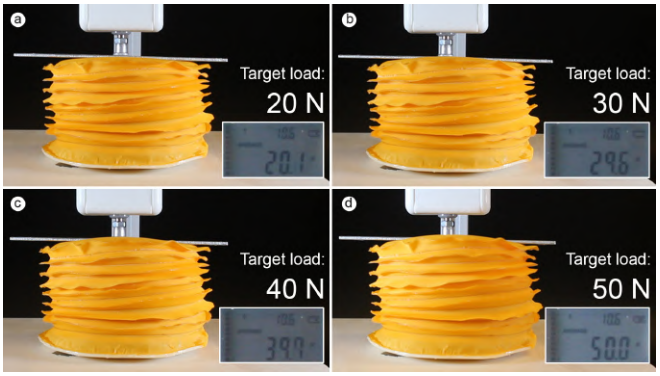

Fig. 9: Results from the control implementation.

This predicted contact force was used as the input for the PID controller, which runs on the Arduino. The output of the PID controller is a pulse-width modulated signal which is used to power an air pump that inflates the bellow. The sampling and actuation interval of the controller was 10 Hz. To allow the system to correct both positive and negative errors from the target contact force, a constant leaking of the bellow was introduced using a valve. A force sensor was placed at a distance of 15 mm above the uninflated module to test the system. Target contact forces were set at 20, 30, 40, and 50 N. The target contact force was then compared to that of the force sensor. The results are shown in Fig. 9. The results are also shown in the supplementary video. It can be seen that the contact force realized by the control system fluctuates around the target force with a maximum error of 2 N. This is in good agreement with the earlier mentioned MSE of 4.73.

V. Conclusions

This study demonstrates a soft robotic module that can sense and control the contact force. The work shows that the shape information provided by the optical sensors in addition to a measurement of the air pressure inside the module provides sufficient information for accurate force prediction. The presented optical sensing method is interesting as it is low-cost, avoids the need for sensors on top of the moving modules, and can sense the contact force as well as the shape.

We envision the use of multiple collaborative modules to realize pressure distribution control in support devices such as seats and mattresses. Therefore, the speed and consistency of the manufacturing process of the individual modules need to be further improved. While the force sensing principle has been validated on a linear actuator, it is expected to be able to predict the loading perpendicular to the top surface also when non-axisymmetric loads occur (e.g. shear loads

in support devices). These various loading conditions will need to be included in the training data. Moreover, future work will present a test setup to correct the over-inflation mentioned in Sec. IV-B. For instance, a second pump could be added to let the extra air out. An addition to the present paper will focus on transferring the learned calibration model of one module to another in order to reduce the time needed for data collection.

REFERENCES

[1] R. Zenk, "Objektivierung des sitzkomforts und seine automatische anpassung," Ph.D. dissertation, TU Munchen, Munchen, November 2008. [Online]. Available: https://mediatum.ub.tum.de/656298

[2] C. Mergl, M. Klendauer, C. Mangen, and H. Bubb, "Predicting long term riding comfort in cars by contact forces between human and seat," in *SAE Technical Paper*. SAE International, 06 2005.

[3] U. Kilincsoy, "Digitalization of posture-based seat design developing car interiors by involving user demands and activities," Ph.D. dissertation, TU Delft, Delft, January 2019. [Online]. Available: http://resolver.tudelft.nl/uuid:419e4678-cb27-4c03-9725-7fb5b0fd3a12

[4] Octaspring, "Octaspring aerospace technology," Available at https://www.octaspringtechnology.com/octaspring-technology/ (2019/08/30).

[5] A. D. Marchese, K. Komorowski, C. D. Onal, and D. Rus, "Design and control of a soft and continuously deformable 2d robotic manipulation system," in *2014 IEEE International Conference on Robotics and Automation (ICRA)*, May 2014, pp. 2189–2196.

[6] M. A. Robertson, M. Murakami, W. M. Felt, J. Paik, M. A. Robertson, W. Felt, and J. Paik, "A compact modular soft surface with reconfigurable shape and stiffness," *IEEE/ASME Transactions on Mechatronics*, vol. 24, no. 1, pp. 16–24, 2018.

[7] C. Larson, B. Peele, S. Li, S. Robinson, M. Totaro, L. Beccai, B. Mazzolai, and R. Shepherd, "Highly stretchable electroluminescent skin for optical signaling and tactile sensing," *Science*, vol. 351, no. 6277, pp. 1071–1074, 2016.

[8] J. Zhou, Y. Gu, P. Fei, W. Mai, Y. Gao, R. Yang, G. Bao, and Z. L. Wang, "Flexible piezotronic strain sensor," *Nano Letters*, vol. 8, no. 9, pp. 3035–3040, 2008.

[9] H. Zhao, K. O'Brien, S. Li, and R. F. Shepherd, "Optoelectronically innervated soft prosthetic hand via stretchable optical waveguides," *Science Robotics*, vol. 1, no. 1, 2016.

[10] I. M. Van Meerbeek, C. M. De Sa, and R. F. Shepherd, "Soft optoelectronic sensory foams with proprioception," *Science Robotics*, vol. 3, no. 24, 2018.

[11] J.-B. Chossat, Y.-L. Park, R. J. Wood, and V. Duchaine, "A soft strain sensor based on ionic and metal liquids," *IEEE Sensors Journal*, vol. 13, no. 9, pp. 3405–3414, 2013.

[12] G. T. Pham, Y.-B. Park, Z. Liang, C. Zhang, and B. Wang, "Processing and modeling of conductive thermoplastic/carbon nanotube films for strain sensing," *Composites Part B: Engineering*, vol. 39, no. 1, pp. 209 – 216, 2008, marine Composites and Sandwich Structures.

[13] R. B. N. Scharff, R. M. Doornbusch, X. L. Klootwijk, A. A. Doshi, E. L. Doubrovski, J. Wu, J. M. P. Geraedts, and C. C. L. Wang, "Color-based sensing of bending deformation on soft robots," in *2018 IEEE International Conference on Robotics and Automation (ICRA)*, May 2018, pp. 1–7.

[14] R. B. N. Scharff, R. M. Doornbusch, E. L. Doubrovski, J. Wu, J. M. P. Geraedts, and C. C. L. Wang, "Color-based proprioception of soft actuators interacting with objects," *IEEE/ASME Transactions on Mechatronics*, vol. 24, no. 5, pp. 1964–1973, Oct 2019.

[15] A. Kadowaki, T. Yoshikai, M. Hayashi, and M. Inaba, "Development of soft sensor exterior embedded with multi-axis deformable tactile sensor system," in *RO-MAN 2009 - The 18th IEEE International Symposium on Robot and Human Interactive Communication*, Sep. 2009, pp. 1093–1098.

[16] K. Vlack, T. Mizota, N. Kawakami, K. Kamiyama, H. Kajimoto, and S. Tachi, "Gelforce: A vision-based traction field computer interface," in *CHI '05 Extended Abstracts on Human Factors in Computing Systems*, ser. CHI EA '05. New York, NY, USA: ACM, 2005, pp. 1154–1155.

[17] M. K. Johnson and E. H. Adelson, "Retrographic sensing for the measurement of surface texture and shape," in *2009 IEEE Conference on Computer Vision and Pattern Recognition*, June 2009, pp. 1070–1077.

[18] X. Lin and M. Wiertlewski, "Sensing the frictional state of a robotic skin via subtractive color mixing," *IEEE Robotics and Automation Letters*, vol. 4, no. 3, pp. 2386–2392, July 2019.

[19] B. Ward-Cherrier, N. Pestell, L. Cramphorn, B. Winstone, M. E. Giannaccini, J. Rossiter, and N. F. Lepora, "The tactip family: Soft optical tactile sensors with 3d-printed biomimetic morphologies," *Soft Robotics*, vol. 5, no. 2, pp. 216–227, 2018, pMID: 29297773.

[20] K. Sato, K. Kamiyama, N. Kawakami, and S. Tachi, "Finger-shaped gelforce: Sensor for measuring surface traction fields for robotic hand," *IEEE Transactions on Haptics*, vol. 3, no. 1, pp. 37–47, Jan 2010.

[21] Y. Sugiura, G. Kakehi, A. Withana, C. Lee, D. Sakamoto, M. Sugimoto, M. Inami, and T. Igarashi, "Detecting shape deformation of soft objects using directional photoreflectivity measurement," in *Proceedings of the 24th Annual ACM Symposium on User Interface Software and Technology*, ser. UIST '11. New York, NY, USA: ACM, 2011, pp. 509–516.

[22] R. B. N. Scharff, J. Wu, J. M. P. Geraedts, and C. C. L. Wang, "Reducing out-of-plane deformation of soft robotic actuators for stable grasping," in *2019 2nd IEEE International Conference on Soft Robotics (RoboSoft)*, April 2019, pp. 265–270.

[23] E. Brown, N. Rodenberg, J. Amend, A. Mozeika, E. Steltz, M. R. Zakin, H. Lipson, and H. M. Jaeger, "Universal robotic gripper based on the jamming of granular material," *Proceedings of the National Academy of Sciences*, vol. 107, no. 44, pp. 18 809–18 814, 2010.

[24] Y. Wei, Y. Chen, T. Ren, Q. Chen, C. Yan, Y. Yang, and Y. Li, "A novel, variable stiffness robotic gripper based on integrated soft actuating and particle jamming," *Soft Robotics*, vol. 3, no. 3, pp. 134–143, 2016.

[25] T. Ranzani, M. Cianchetti, G. Gerboni, I. D. Falco, G. Petroni, and A. Menciassi, "A modular soft manipulator with variable stiffness," 3rd joint workshop on new technologies for computer/robot assisted surgery, 2013.

[26] J. Ou, L. Yao, D. Tauber, J. Steimle, R. Niiyama, and H. Ishii, "jamsheets: Thin interfaces with tunable stiffness enabled by layer jamming," 02 2014, pp. 65–72.

[27] Y.-F. Zhang, N. Zhang, H. Hingorani, N. Ding, D. Wang, C. Yuan, B. Zhang, G. Gu, and Q. Ge, "Fast-response, stiffness-tunable soft actuator by hybrid multimaterial 3d printing," *Advanced Functional Materials*, vol. 29, no. 15, p. 1806698, 2019.

[28] A. Stilli, H. A. Wurdemann, and K. Althoefer, "Shrinkable, stiffness-controllable soft manipulator based on a bio-inspired antagonistic actuation principle," in *2014 IEEE/RSJ International Conference on Intelligent Robots and Systems*, Sep. 2014, pp. 2476–2481.

[29] R. B. N. Scharff, E. L. Doubrovski, W. A. Poelman, P. P. Jonker, C. C. L. Wang, and J. M. P. Geraedts, "Towards behavior design of a 3d-printed soft robotic hand," in *Soft Robotics: Trends, Applications and Challenges*, C. Laschi, J. Rossiter, F. Iida, M. Cianchetti, and L. Margheri, Eds. Cham: Springer International Publishing, 2017, pp. 23–29.

[30] F. Maghooa, A. Stilli, Y. Noh, K. Althoefer, and H. A. Wurdemann, "Tendon and pressure actuation for a bio-inspired manipulator based on an antagonistic principle," in *2015 IEEE International Conference on Robotics and Automation (ICRA)*, May 2015, pp. 2556–2561.

[31] M. Manti, V. Cacucciolo, and M. Cianchetti, "Stiffening in soft robotics: A review of the state of the art," *IEEE Robotics Automation Magazine*, vol. 23, no. 3, pp. 93–106, Sep. 2016.

[32] H. D. Yang and A. T. Asbeck, "A new manufacturing process for soft robots and soft/rigid hybrid robots," in *2018 IEEE/RSJ International Conference on Intelligent Robots and Systems (IROS)*. IEEE, 2018, pp. 8039–8046.